AD-A044 619 POLYTECHNIC INST OF NEW YORK FARMINGDALE DEPT OF MEC--ETC F/G 20/4
COMPUTATION OF SHOCK LAYERS ABOUT ABLATED, BLUNT-NOSED BODIES.(U)
AUG 77 G MORETTI N00014-75-C-0511
UNCLASSIFIED POLY-M/AE-77-14 NL

1 OF 1
ADA044619

END
DATE FILMED
10-77
DDC

Polytechnic Institute of New York

AERODYNAMICS LABORATORIES

DEPARTMENT OF MECHANICAL and AEROSPACE ENGINEERING

12 P.G.

COMPUTATION OF SHOCK LAYERS ABOUT ABLATED, BLUNT-NOSED BODIES

by GINO MORETTI

AUGUST 1977

CONTRACT NO. N00014-75-C-0511
PROJECT NO. NR 061-135

POLY-M/AE Report No. 77-14

Unclassified

SECURITY CLASSIFICATION OF THIS PAGE (When Data Entered)

REPORT DOCUMENTATION PAGE	READ INSTRUCTIONS BEFORE COMPLETING FORM
1. REPORT NUMBER: POLY-M/AE ~~Report~~ No. 77-14	2. GOVT ACCESSION NO.
3. RECIPIENT'S CATALOG NUMBER	
4. TITLE (and Subtitle): COMPUTATION OF SHOCK LAYERS ABOUT ABLATED, BLUNT-NOSED BODIES.	5. TYPE OF REPORT & PERIOD COVERED: Scientific Interim
6. PERFORMING ORG. REPORT NUMBER	
7. AUTHOR(s): GINO MORETTI	8. CONTRACT OR GRANT NUMBER(s): N00014-75-C-0511
9. PERFORMING ORGANIZATION NAME AND ADDRESS: Polytechnic Institute of New York, Aerodynamics Laboratories, Route 110, Farmingdale, N.Y. 11735	10. PROGRAM ELEMENT, PROJECT, TASK AREA & WORK UNIT NUMBERS: NR 061-135
11. CONTROLLING OFFICE NAME AND ADDRESS: Office of Naval Research, Department of the Navy, Arlington, VA 22217	12. REPORT DATE: August 1977
	13. NUMBER OF PAGES: 41
14. MONITORING AGENCY NAME & ADDRESS (if different from Controlling Office)	15. SECURITY CLASS. (of this report): Unclassified
	15a. DECLASSIFICATION/DOWNGRADING SCHEDULE

16. DISTRIBUTION STATEMENT (of this Report)

Approved for public release; distribution unlimited.

17. DISTRIBUTION STATEMENT (of the abstract entered in Block 20, if different from Report)

18. SUPPLEMENTARY NOTES

19. KEY WORDS (Continue on reverse side if necessary and identify by block number)

Numerical gas dynamics
Ablated bodies
Blunt bodies
Compressible flow

20. ABSTRACT (Continue on reverse side if necessary and identify by block number)

A technique is described to calculate steady, inviscid, supersonic flows past blunt-nosed vehicles affected by ablation. New computational grids are created by conformal mapping. Stretching of coordinates for further application to viscous flows is demonstrated. The technique does not apply to flows with imbedded shocks.

DD FORM 1 JAN 73 1473 EDITION OF 1 NOV 65 IS OBSOLETE

410 338

Unclassified

SECURITY CLASSIFICATION OF THIS PAGE (When Data Entered)

COMPUTATION OF SHOCK LAYERS ABOUT ABLATED, BLUNT-NOSED BODIES

by

Gino Moretti

This research was conducted under the sponsorship of the Office of Naval Research under Contract No. N00014-75-C-0511, Project No. NR 061-135.

POLYTECHNIC INSTITUTE OF NEW YORK

Aerodynamics Laboratories

August 1977

POLY-M/AE Report No. 77-14

COMPUTATION OF SHOCK LAYERS ABOUT ABLATED, BLUNT-NOSED BODIES[†]

by

Gino Moretti[‡]

Polytechnic Institute of New York
Aerodynamics Laboratories
Farmingdale, New York

ABSTRACT

A technique is described to calculate steady, inviscid, supersonic flows past blunt-nosed vehicles affected by ablation. New computational grids are created by conformal mapping. Stretching of coordinates for further application to viscous flows is demonstrated. The technique does not apply to flows with imbedded shocks.

[†]This research was conducted under the sponsorship of the Office of Naval Research under Contract No. N00014-75-C-0511, Project No. NR 061-135.

[‡]Professor, Dept. of Mechanical and Aerospace Engineering.

TABLE OF CONTENTS

TABLE OF CONTENTS (Contd.)

LIST OF ILLUSTRATIONS

1. Introduction

A computational technique is described in the present paper, to evaluate steady, inviscid, compressible flows past certain vehicles flying at supersonic speed. The object of the analysis is twofold:

1) to provide a tool for an accurate evaluation of inviscid blunt body flows, even in the presence of imbedded shocks, and of flows about afterbodies whose cross-sections are not far from circles but whose longitudinal sections are substantially different from sections of cones or cylinders (a typical situation occurring in vehicles originally designed as cones, bicones, cones-cylinders, as a consequence of ablation); and

2) to provide a reliable basic computational tool for a further extension to the analysis of viscous flows.

Since departure from axially symmetric geometries is assumed to be not too strong (as opposed to geometries of aircraft, see Ref. 1), we will stipulate to build our analysis around a basic cylindrical frame of reference, whose axis (to be called x) lies in the general direction of the length of the vehicle. Meridional planes, defined by an angle φ, contain identical flows if the geometry is axially symmetric and the angle of attack is zero. Three-dimensional flows

will be analyzed by adding three-dimensional effects (along the φ-coordinate) to a basic axisymmetric analysis. The latter will thus be considered our initial goal, for the sake of simplicity, and will be described in the present paper. We will also limit the analysis to flows without imbedded shocks. Extensions of the technique to flow with shocks and three-dimensional flows will be discussed elsewhere.

2. Generalities and Nomenclature

Let x be the axis of symmetry of the vehicle, and y the radial coordinate in any meridional plane (x and y here stand for the more familiar z and r of a cylindrical coordinate system). Let $\hat{I}$ and $\hat{J}$ be the unit vectors in the x- and y-direction, respectively. As usual (Ref. 1), we will choose $P=\ln(p/p_\infty)$ and S as thermodynamical unknowns (where S is the entropy measured from its value at infinity, divided by c_v) and

$$\vec{V} = U\hat{I} + V\hat{J} \qquad (1)$$

to represent the unknown velocity vector which, as well as its modulus q, will be considered in multiples of $(p_\infty/\rho_\infty)^{\frac{1}{2}}$. In addition, we will make use of γ, the ratio of specific heats, and of the variable, nondimensional temperature,

$$\mathcal{T} = \frac{p/p_\infty}{\rho/\rho_\infty} \qquad (2)$$

Lengths will be scaled to a reference value, x_{ref}, typical of the vehicle.

Two problems will be examined:

1) the evaluation of the steady, transonic flow past the blunt nose of the vehicle, for which a time-dependent computational technique will be used, and

2) the evaluation of the steady, supersonic flow about the afterbody, for which a marching computational technique will be used.

When time-dependent calculations are performed, all times will be scaled to a reference time, $t_{ref}=x_{ref}/(p_\infty/\rho_\infty)^{\frac{1}{2}}$.

The equations of motion are, then, conveniently written in the form:

$$\left.\begin{aligned} P_t+\vec{V}\cdot\nabla P+\gamma\nabla\cdot\vec{V}+j\gamma\frac{V}{y} &= 0 \\ \vec{V}_t+\tfrac{1}{2}\nabla q^2-\vec{V}\times\nabla\times\vec{V}+\tfrac{1}{\rho}\nabla P &= 0 \\ S_t+\vec{V}\cdot\nabla S &= 0 \end{aligned}\right\} \qquad (3)$$

where j=1 for axisymmetric flows. The same system may be used for two-dimensional problems by simply letting j=0. It is also clear that steady problems are defined by (3) after dropping all time derivatives.

3. Computational Frame and Basic Equations of Motion

Most of the calculations of blunt body and afterbody flows have been performed, in the last decade, using a cylindrical frame such as the one described above, or a spherical frame, and in many cases the results have been excellent. Calculations about bodies with concavities, such as ablated cones or bodies with flares, may not be equally successful, primarily because the computational grid cannot be properly adjusted to the body geometry. It is well-known, indeed, that one of the grid lines should intersect the body under an angle as close as possible to a right angle, in order to improve accuracy.

Therefore, following the same line of thought as exposed in Ref. 1, but in meridional planes rather than in cross-sectional planes, we will recast the equations of motion in another, curvilinear, frame defined by two variables, ξ and η, such that the image of the body in the (ξ,η)-plane be as close as possible to an η-constant line. To this effect, we will use a conformal mapping to represent the correspondence between the complex z-plane, where

$$z = x+iy \tag{4}$$

and the complex ζ-plane, where

$$\zeta = \xi+i\eta \tag{5}$$

Details on the nature of the conformal mapping will be given later on (in Section 14). We can provide, however, a large number of general formulas, valid regardless of the particular mapping being used.

Let $\hat{i}$ and $\hat{j}$ be the unit vectors (in the z-plane) parallel to the η=constant line and to the ξ=constant line, respectively. Let us also define new velocity components, u and v, by

$$\vec{V} = u\hat{i}+v\hat{j} \tag{6}$$

Let us also define

$$g = \frac{d\zeta}{dz} = Ge^{i\omega} \tag{7}$$

$$\varphi = \frac{1}{g}\frac{d \log g}{dz} = \varphi_1 + i\varphi_2 \tag{8}$$

and

$$\mathcal{C}+i\mathcal{S} = \frac{G}{g} = e^{-i\omega} \tag{9}$$

It is convenient to note that

$$\xi_x=G\mathcal{C} \ , \ \xi_y=G\mathcal{S} \ , \ \eta_x=-G\mathcal{S} \ , \ \eta_y=G\mathcal{C} \tag{10}$$

$$x_\xi=\mathcal{C}/G \ , \ x_\eta=-\mathcal{S}/G \ , \ y_\xi=\mathcal{S}/G \ , \ y_\eta=\mathcal{C}/G \tag{11}$$

$$\xi_x^2+\xi_y^2=G^2 \ , \ x_\xi^2+x_y^2=1/G^2 \tag{12}$$

$$G_\xi=G\varphi_1 \ , \ G_\eta=-G\varphi_2 \ , \ \omega_\xi=\varphi_2 \ , \ \omega_\eta=\varphi_1 \tag{13}$$

$$\hat{i}\cdot\hat{I}=\mathcal{C} \ , \ \hat{i}\cdot\hat{J}=\mathcal{S} \ , \ \hat{j}\cdot\hat{I}=-\mathcal{S} \ , \ \hat{j}\cdot\hat{J}=\mathcal{C} \tag{14}$$

$$U=u\mathcal{C}-v\mathcal{S} \ , \ V=u\mathcal{S}+v\mathcal{C} \ , \ u=U\mathcal{C}+V\mathcal{S} \ , \ v=-U\mathcal{S}+V\mathcal{C} \tag{15}$$

The basic vector operators in (3) can be expressed as follows:

$$\left.\begin{aligned} &\nabla P = G\left(P_\xi \hat{i} + P_\eta \hat{j}\right) \\ &\nabla \times \vec{V} = G^2\left[\left(\frac{v}{G}\right)_\xi - \left(\frac{u}{G}\right)_\eta\right]\hat{k} \\ &\vec{V} \times \nabla \times \vec{V} = G^2\left[\left(\frac{v}{G}\right)_\xi - \left(\frac{u}{G}\right)_\eta\right](v\hat{i} - u\hat{j}) \\ &\nabla \cdot \vec{V} = G^2\left[\left(\frac{u}{G}\right)_\xi + \left(\frac{v}{G}\right)_\eta\right] \end{aligned}\right\} \qquad (16)$$

so that (3) become:

$$\left.\begin{aligned} &P_\tau + GuP_\xi + GvP_\eta + \gamma Gu_\xi + \gamma Gv_\eta - \gamma(uG_\xi + vG_\eta) + j\gamma\,\frac{V}{y} = 0 \\ &u_\tau + Guu_\xi + Gvu_\eta + v^2 G_\xi - uvG_\eta + \mathcal{J}GP_\xi = 0 \\ &v_\tau + Guv_\xi + Gvv_\eta - uvG_\xi + u^2 G_\eta + \mathcal{J}GP_\eta = 0 \\ &S_\tau + G(uS_\xi + vS_\eta) = 0 \end{aligned}\right\} \qquad (17)$$

where τ has been used instead of t, although derivatives with respect to t and with respect to τ are identical, since the mapping does not depend on time.

We will now make use of (13) and introduce the notations:

$$D = v\varphi_1 + u\varphi_2 \ , \quad E = -u\varphi_1 + v\varphi_2 + j\,\frac{V}{Gy} \qquad (18)$$

to rewrite (17) in the simpler form:

$$\left.\begin{aligned} &P_\tau + G(uP_\xi + vP_\eta + \gamma u_\xi + \gamma v_\eta + \gamma E) = 0 \\ &u_\tau + G(uu_\xi + vu_\eta + vD + \mathcal{J}P_\xi) = 0 \\ &v_\tau + G(uv_\xi + vv_\eta - uD + \mathcal{J}P_\eta) = 0 \\ &S_\tau + G(uS_\xi + vS_\eta) = 0 \end{aligned}\right\} \qquad (19)$$

4. Coordinate Stretching and Final Equations of Motion

In viscous flow problems, a strong concentration of grid lines near the body is necessary, to describe the boundary layer with sufficient resolution, and it can be achieved by stretching the η-coordinate. We will define a stretching function depending on one parameter, α; values of α less than 1 produce almost undetectable stretchings, whereas the concentration of grid lines near the body can be made as great as necessary by using sufficiently large values of α.

In general, let

$$\eta = b(\xi) \tag{20}$$

and

$$\eta = c(\xi,t) \tag{21}$$

be the equations of the images of the body and of the shock in the ζ-plane. We will define a new coordinate, X, as follows:

$$X=1+\frac{1}{\alpha}\,\text{argtanh}\,\frac{\eta-c}{\delta}\ ,\quad \eta=c+\delta\tanh[\alpha(X-1)] \tag{22}$$

where

$$\delta = \frac{c-b}{\tanh\,\alpha} \tag{23}$$

Therefore,

$$X_\eta = \frac{\delta}{\alpha[\delta^2-(\eta-c)^2]} \tag{24}$$

$$X_\xi = -\left[\frac{\eta - c}{\mathcal{J}\tanh\alpha}(c_\xi - b_\xi) + c_\xi\right]X_\eta \tag{25}$$

$$X_t = -\left[\frac{\eta - c}{\mathcal{J}\tanh\alpha} + 1\right]c_\tau X_\eta \tag{26}$$

Letting $Y=\xi$, $T=\tau$,

$$A = X_\tau + GuX_\xi + GvX_\eta \tag{27}$$

the equations of motion (19) become

$$\left.\begin{aligned} &P_T + AP_X + G(uP_Y + \gamma u_Y + \gamma X_\xi u_X + \gamma X_\eta v_X + \gamma E) = 0 \\ &u_T + Au_X + G(uu_Y + vD + \mathcal{J}P_Y + \mathcal{J}X_\xi P_X) = 0 \\ &v_T + Av_X + G(uv_Y - uD + \mathcal{J}X_\eta P_X) = 0 \\ &S_T + AS_X + GuS_Y = 0 \end{aligned}\right\} \tag{28}$$

Note that, at the body, $\eta=b$, $X=0$, $X_\eta = \cosh^2\alpha/\alpha\mathcal{J}$, $X_\xi = -b_\xi X_\eta$, $X_\tau = 0$, and, at the shock, $\eta=c$, $X=1$, $X_\eta = 1/\alpha\mathcal{J}$, $X_\xi = -c_\xi X_\eta$, $X_\tau = -c_t X_\eta$.

In general,

$$\xi_X = 0,\quad \xi_Y = 1,\quad \xi_T = 0,\quad \eta_X = 1/X_\eta,\quad \eta_Y = -X_\xi/X_\eta,\quad \eta_T = -X_\tau/X_\eta. \tag{29}$$

5. Characteristic Equation for the Time-Dependent Problem

To evaluate points on the body surface or on the bow shock, a characteristic equations in X and T, obtained from the first three equations (28), is needed. With

$$\left.\begin{aligned} R_1 &= uP_Y + \gamma u_Y + \gamma E \\ R_2 &= uu_Y + vD + \mathcal{J}P_Y \\ R_3 &= uv_Y - uD \end{aligned}\right\} \tag{30}$$

a linear combination of the first three equations (28) is written in the form:

$$\mu_1 (P_T+\lambda P_X)+\mu_2 (u_T+\lambda u_X)+\mu_3 (v_T+\lambda v_X)+G \sum_1^3 \mu_i R_i = 0 \qquad (31)$$

whose λ turns out to be defined by

$$\lambda=A\pm aG\sqrt{X_\xi^2+X_\eta^2} \qquad (32)$$

and, consequently,

$$\mu_1=A-\lambda, \quad \mu_2=-\gamma G X_\xi, \quad \mu_3=-\gamma G X_\eta \qquad (33)$$

6. Body Calculation for the Time-Dependent Problem

At body points, λ is defined by the lower sign in (32) and A=0. The boundary condition yields:

$$\vec{V}\cdot\hat{N} = uN_1+vN_2 = 0 \qquad (34)$$

where $\hat{N}=N_1\hat{i}+N_2\hat{j}$ is the unit vector normal to the body. Since

$$\hat{N} = \frac{-dy\hat{I}+dx\hat{J}}{(dx^2+dy^2)^{1/2}} \qquad (35)$$

(11), (12), (14) and (20) can be applied, to obtain

$$\begin{aligned} -dy\hat{I}+dx\hat{J} &= -(y_\xi d\xi+y_\eta d\eta)\hat{I}+(x_\xi d\xi+x_\eta d\eta)\hat{J} \\ &= \frac{1}{G}\left[-(\mathcal{L}d\xi+\mathcal{C}d\eta)\hat{I}+(\mathcal{C}d\xi-\mathcal{L}d\eta)\hat{J}\right] \\ &= \frac{1}{G}\left[-d\eta\hat{i}+d\xi\hat{j}\right] \end{aligned}$$

$$N_2=\frac{1}{\nu}, \quad N_1=-b_\xi N_2, \quad \nu=\sqrt{1+b_\xi^2} \qquad (36)$$

It follows that

$$-ub_{\xi}+v = 0 \tag{37}$$

and

$$-u_T b_{\xi}+v_T = 0 \tag{38}$$

By replacing (33) into (31) and taking (38) into account, one obtains:

$$-\lambda(P_T+\lambda P_X)+\lambda\gamma X_{\eta}(b_{\xi}u_X-v_X)+\Sigma u_i R_i=0$$

Therefore, the pressure is defined by:

$$P_T=-\lambda P_X+\gamma G X_{\eta}(b_{\xi}u_X-v_X)+\frac{G}{\lambda}\Sigma u_i R_i \tag{39}$$

The entropy is obviously constant at the body, if initially assumed equal to the stagnation entropy. The velocity can be computed as follows: Let

$$\tilde{v} = u+vb_{\xi}=u\nu^2 \tag{40}$$

Multiply the third of (28) by b_{ξ} and add to the second. At the body,

$$u_T+v_T b_{\xi}+G[u(u_Y+v_Y b_{\xi})+\mathcal{J}P_Y] = 0$$

which, since

$$\tilde{v}_T = u_T+v_T b_{\xi}$$

$$\tilde{v}_Y=u_Y+v_Y b_{\xi}+vb_{\xi\xi}$$

can be written as

$$\tilde{v}_T+G[u(\tilde{v}_Y-vb_{\xi\xi})+\mathcal{J}P_Y] = 0 \tag{41}$$

This equation yields $\tilde{v}$; afterwards, u and v follow from

$$u=\tilde{v}/\nu^2 \quad , \quad v=ub_\xi \tag{42}$$

To evaluate b_ξ and $b_{\xi\xi}$, if the body is defined by a function y(x) in the physical plane, we note that

$$\frac{db}{d\xi} = \frac{b_x+b_y y'}{\xi_x+\xi_y y'} = \frac{-\zeta+\mathcal{C}y'}{\mathcal{C}+\zeta y'} \tag{43}$$

by virtue of (10), if $y'=dy/dx$. A further differentiation yields

$$\frac{d^2b}{d\xi^2} = [-\zeta_\xi+\mathcal{C}_\xi y'+\mathcal{C}y''x_\xi - \frac{db}{d\xi}(\mathcal{C}_\xi+\zeta_\xi y'+\zeta y''x_\xi)]/(\mathcal{C}+\zeta y')$$

so that, by taking (9), (11) and (13) into account,

$$\frac{d^2b}{d\xi^2} = \frac{(1+y'^2)\varphi_2+\mathcal{C}y''/G}{(\mathcal{C}+\zeta y')^2} \tag{44}$$

7. Bow Shock Calculation for the Time-Dependent Problem

To compute the bow shock in the time-dependent problem, we define the unit vector normal to the shock, N, as

$$\hat{N} = N_1\hat{i} + N_2\hat{j} \tag{45}$$

By arguments similar to the ones leading to (36), we obtain:

$$N_2=1/\nu \quad , \quad N_1=-c_\xi N_2 \quad , \quad \nu=\sqrt{1+c_\xi^2} \tag{46}$$

Note, however, that c depends on t as well as on ξ. Therefore,

$$\nu_T=c_\xi c_{\xi T}/\nu = c_Y c_{YT}/\nu \tag{47}$$

$$N_{2T}=-\nu_T/\nu^2 \quad , \quad N_{1T}=-c_{YT}/\nu+c_Y\nu_T/\nu^2 \tag{48}$$

The free-stream velocity, for an axisymmetric flow, must be parallel to the x-axis. Consequently,

$$\left.\begin{aligned} u_\infty &= U_\infty \mathcal{C} \\ v_\infty &= -U_\infty \mathcal{S} \end{aligned}\right\} \qquad \left.\begin{aligned} u_{\infty T} &= -v_\infty \omega_T \\ v_{\infty T} &= u_\infty \omega_T \end{aligned}\right\} \tag{49}$$

If Q is a point on the shock, the velocity of the shock, W, is given by

$$W = \frac{dQ}{dt}\cdot\hat{N} = (x_Q)_t \hat{I}\cdot\hat{N} + (y_Q)_t \hat{J}\cdot\hat{N} \tag{50}$$

but

$$(x_Q)_t + i(y_Q)_t = (z_Q)_t = \frac{1}{g}(\zeta_Q)_t \tag{51}$$

Now, let Q be a point which remains on the same ξ=constant line, as the shock moves. Therefore,

$$(x_Q)_t + i(y_Q)_t = \frac{i}{g} c_t \tag{52}$$

From (52) and (50), using (45) and (14), we obtain

$$W = \frac{1}{G} N_2 c_T \tag{53}$$

Let $\tilde{u}$ be the velocity component normal to the shock, and

$$\tilde{u}_{rel} = \tilde{u} - W \tag{54}$$

Consequently,

$$\tilde{u}_{\infty rel} = u_\infty N_1 + (v_\infty - \frac{1}{G} c_T) N_2 \tag{55}$$

and

$$(\tilde{u}_{\infty rel})_T = -v_\infty N_{1\omega T} + u_\infty N_{1T} + (u_\infty \omega_T + \frac{1}{G^2} G_T c_T - \frac{1}{G} c_{TT}) N_2 + (v_\infty - \frac{1}{G} c_T) N_{2T} \tag{56}$$

Note that $\omega_t = 0$ but

$$\omega_T = -\varphi_1 \frac{X_t}{X_\eta} = \varphi_1 c_T \tag{57}$$

at the shock. Similarly,

$$G_T = -\varphi_2 c_T G \tag{58}$$

We will write (56) in the form:

$$(u_{\infty rel})_T = C_1 c_{TT} + C_2 \tag{59}$$

by letting

$$C_1 = -N_2/G \tag{60}$$

$$C_2 = (u_\infty N_2 - v_\infty N_1)\omega_T + u_\infty N_{1T} + (v_\infty - \frac{1}{G} c_T) N_{2T} + \varphi_2 c_T^2 C_1 \tag{61}$$

We write now the Rankine-Hugoniot conditions in the form:

$$P = \ell n \frac{2}{\gamma+1} + \ell n (\tilde{u}^2_{\infty rel} - \frac{\gamma-1}{2}) \tag{62}$$

$$\tilde{u}_{rel} = \frac{\gamma-1}{\gamma+1} \tilde{u}_{\infty rel} + \frac{2\gamma}{\gamma+1} \frac{1}{\tilde{u}_{\infty rel}} \tag{63}$$

By differentiation with respect to T, and by letting

$$D_1 = \frac{2\tilde{u}_{\infty rel}}{\tilde{u}^2_{\infty rel} - \frac{\gamma-1}{2}}, \quad D_2 = \frac{\gamma-1}{\gamma+1} - \frac{2\gamma}{\gamma+1} \frac{1}{\tilde{u}^2_{\infty rel}} \tag{64}$$

we obtain from (62) and (63):

$$P_T = C_3 c_{TT} + C_4 \tag{65}$$

$$(\tilde{u}_{rel})_T = C_5 c_{TT} + C_6 \tag{66}$$

with

$$C_3 = D_1 C_1 \quad , \quad C_4 = D_1 C_2 \tag{67}$$

$$C_5 = D_2 C_1 \quad , \quad C_6 = D_2 C_2 \tag{68}$$

Since

$$(\tilde{u} - \tilde{u}_\infty)_T = (\tilde{u}_{rel} - \tilde{u}_{\infty\, rel})_T \tag{69}$$

from (59) and (66) it follows that

$$(\tilde{u} - \tilde{u}_\infty)_T = C_9 c_{TT} + C_{10} \tag{70}$$

with

$$C_9 = C_5 - C_1 \quad , \quad C_{10} = C_6 - C_2 \tag{71}$$

Because of the conservation of the velocity component tangent to the shock,

$$\vec{V} = \vec{V}_\infty + (\tilde{u} - \tilde{u}_\infty)\hat{N} \tag{72}$$

if V is the velocity immediately behind the shock. Therefore,

$$\left.\begin{aligned} u &= u_\infty + (\tilde{u} - \tilde{u}_\infty) N_1 \\ v &= v_\infty + (\tilde{u} - \tilde{u}_\infty) N_2 \end{aligned}\right\} \tag{73}$$

and

$$\left.\begin{aligned} u_T &= C_{11} c_{TT} + C_{12} \\ v_T &= C_{13} c_{TT} + C_{14} \end{aligned}\right\} \tag{74}$$

with

$$\left.\begin{aligned} C_{11} &= C_9 N_1 \\ C_{13} &= C_9 N_2 \end{aligned}\right\} \qquad \left.\begin{aligned} C_{12} &= -v_\infty {}^{W}_{T} + C_{10} N_1 + (\tilde{u} - \tilde{u}_\infty) N_{1T} \\ C_{14} &= u_\infty {}^{W}_{T} + C_{10} N_2 + (\tilde{u} - \tilde{u}_\infty) N_{2T} \end{aligned}\right\} \tag{75}$$

We use now the characteristic equation (31) with λ defined by (32) with the upper sign, and consequently

$$\mu_1 = A - \lambda \quad , \quad \mu_2 = \gamma G X_\eta c_\xi \quad , \quad \mu_3 = -\gamma G X_\eta \tag{76}$$

By replacing (74), (75) and (65) into it, and letting

$$\begin{aligned} D_7 &= 1/(\mu_1 C_3 + \mu_2 C_{11} + \mu_3 C_{13}) \\ D_8 &= \mu_1 C_4 + \mu_2 C_{12} + \mu_3 C_{14} \\ D_9 &= G \Sigma \mu_i R_i \\ \Pi &= \lambda (\mu_1 P_X + \mu_2 u_X + \mu_3 v_X) \end{aligned} \tag{77}$$

the following equation is obtained, to define c_{TT}:

$$c_{TT} = -D_7 (D_8 + D_9 + \Pi) \tag{78}$$

8. Outline of the Computational Program for the Time-Dependent Problem

The steady flow about the blunt nose of the vehicle is determined as the asymptotic solution of an unsteady flow problem. A computational region is chosen, subject to the only condition that the sonic line, as anticipated in the steady state, must lie entirely inside it. A guess is made

for the initial standoff distance of the bow shock, d_o, as a multiple of the nose radius, as follows:

$$d_o = 2.7687/(M_\infty^3 - 1) + .36 \quad \text{for two-dimensional flows} \tag{79}$$

$$d_o = 0.6137/(M_\infty^2 - 1) + .13 \quad \text{for axisymmetric flows} \tag{80}$$

After evaluating the image of the normal shock point in the ζ-plane, the other shock points are assumed to have the same η-coordinate as the former. A computational grid can be defined now, and the shape of the shock in the physical plane can be found. We assume that the shock is initially at rest; therefore, $c_T=0$, $W=0$. The normal to the shock at each point is defined by (45) and (46), the free stream velocity components by the first set in (49) and (55) can be used, with $c_T=0$. Pressure and velocity behind the initial shock are then defined by (62), (63) and (73), whereas the entropy follows from

$$S = P - \gamma \ell n (\tilde{u}_\infty / \tilde{u})_{rel} \tag{81}$$

The entropy on the body surface is assumed equal to the stagnation entropy and initial guesses for P and the modulus of the velocity on the body are made, assuming a Mach number distribution along the body and using well-known expressions for steady, isentropic flow. The two velocity components along the body are obtained by applying the kinematic boundary

condition, that is, vanishing of the normal velocity component. Values of P, S, u and v at all other grid points are initially prescribed by linearly interpolating between body and shock.

Each computational step consists of a predictor level and a corrector level.

Predictor level.

Given original values of P, S, u, v, $\mathcal{J}$, c, c_T, z, ζ, g and φ,

At all values of ξ, compute c_Y, c_{YT}.

At all values of ξ and η,

compute X- and Y-derivatives of P, S, u, v (see next section)

compute X_ξ, X_η, X_t

compute G, A, D, E.

For all points except body and shock points, determine P_T, S_T, u_T and v_T from (28).

For body points, compute R_1, R_2, R_3 from (30), λ from (32), and ω_1, ω_2, ω_3 from (33). Then, use (39) to obtain P_T, (41) to obtain $\tilde{v}_T$ and set $S_T=0$.

For shock points, compute R_1, R_2, R_3 from (30), evaluate N_1 and N_2 from (46) and compute all coefficients (C_1 through C_{14}). Compute D_7, D_8, D_9 and Π and determine c_{TT} from (78).

Update P, S, u, v at all interior points, P and $\tilde{v}$ at all body points, as well as c_T and c, using the following rule (where Φ is an arbitrary function:

$$\tilde{\varphi}(T+\Delta T) = \tilde{\varphi}(T)+\tilde{\varphi}_T\Delta T \tag{82}$$

From the new geometry of the shock (determined by the updated values of c) determine the basic parameters for a new mapping. From the updated values of c, determine new values of c_Y, and new values of N_1, N_2. Then, new values of $u_{\infty\,rel}$ are determined and (62), (63), (73), (81) used to evaluate P, u, v, S behind the shock. Values of $\mathcal{J}$ are now computed throughout by using:

$$\mathcal{J} = \exp\left(\frac{\gamma-1}{\gamma} P+ \frac{1}{\gamma} S\right) \tag{83}$$

Symmetry conditions are imposed where necessary. The initial values of P, S, u, v are temporarily saved.

A new grid (consistent with the new shock location) is computed, including the values of g and φ.

Corrector level.

The computation is restarted as at the beginning of the predictor stage, using all new values. The updating is now performed using the following rule in lieu of (82):

$$\tilde{\varphi}(T+\Delta T)= \frac{1}{2}\left[\tilde{\varphi}(T)+\bar{\tilde{\varphi}}(T+\Delta T)+\tilde{\varphi}_T\Delta T\right] \tag{84}$$

where $\bar{\tilde{\varphi}}(T+\Delta T)$ is the left-hand side of (82) and $\tilde{\varphi}_T$ is the T-derivative computed in the corrector stage. The computational grid must be re-evaluated since the bow shock location may have changed slightly. The values at the shock themselves have to be recomputed as at the end of the predictor

level. Symmetry conditions are imposed again. Finally, the updated values of P, S, u, v, $\mathcal{J}$, c and c_T are stored as initial values for a new step.

9. Discretization of X- and Y-Derivatives

In principle, the MacCormack scheme (Ref. 2) for integrating the equations of motion at all interior points is adopted. This policy is reflected by the use of (82) and (84) at the predictor and corrector level, respectively. In addition, whenever possible, the X- and Y-derivatives should be approximated by 2-point differences taken, for example, forwards at the predictor level and backwards at the corrector level.

There are several exceptions to the above rule:

1) At body boundary points, where X=0, backward approximations cannot be taken and are replaced by the approximation:

$$\phi_X \approx (-2\phi_o + 3\phi_1 - \phi_2)/\Delta X \tag{85}$$

which maintains a second order accuracy if the equations are linear throughout the integration step (Ref. 3). Here, $\phi_i = \phi(i\Delta X, Y)$.

2) Similarly, at shock points, where X=1, forward approximations cannot be taken and are replaced by the approximation:

$$\phi_X \approx (2\phi_o - 3\phi_1 + \phi_2)/\Delta X \tag{86}$$

where $\phi_i = \phi(1 - i\Delta X, \Delta Y)$.

3) The last of (28) simply expresses the fact that entropy is transported unaltered by the moving particles. That means that no entropy signal travels backwards along a particle path. Consequently, no approximations to X- or Y-derivatives are allowed which imply forward differences of S along a particle path. Violation of this physical principle, as a consequence of straightforward application of the MacCormack scheme, affects the results along the symmetry streamline in a blunt body problem, and neighboring points are also affected consequently, with an overall unnecessary lengthening of the computational time for reaching a steady state (Ref. 4). It is therefore advisable to adopt the following scheme systematically:

$$\left.\begin{aligned} &\text{Predictor level:} \quad S_X \approx \mathrm{sgn}A \,\frac{2S_{00}-3S_{10}+S_{20}}{\Delta X}\,, \\ &\qquad\qquad\qquad\quad S_Y \approx \mathrm{sgn}u \,\frac{2S_{00}-3S_{01}+S_{02}}{\Delta Y} \\ &\text{Corrector level:} \quad S_X \approx \mathrm{sgn}A \,\frac{S_{00}-S_{10}}{\Delta X}\,, \\ &\qquad\qquad\qquad\quad S_Y \approx \mathrm{sgn}u \,\frac{S_{00}-S_{01}}{\Delta Y} \end{aligned}\right\} \qquad (87)$$

where

$$\left.\begin{aligned} &S_{00}=S(X,Y)\ ,\ S_{10}=S(X-\Delta X\,\mathrm{sgn}A,Y) \\ &S_{20}=S(X-2\Delta X\,\mathrm{sgn}A,Y) \\ &S_{01}=S(X,Y-\Delta Y\,\mathrm{sgn}u)\ ,\ S_{02}=S(X,Y-2\Delta Y\,\mathrm{sgn}u) \end{aligned}\right\} \qquad (88)$$

4) Similarly, the terms $\tilde{v}_T+Gu\tilde{v}_Y$ in (41) express the Lagrangian derivative of $\tilde{v}$. Forward differencing of $\tilde{v}$ is forbidden and $\tilde{v}_Y$ should be approximated as follows:

$$\left.\begin{aligned} &\text{Predictor level:} \quad \tilde{v}'_Y \approx (\tilde{v}_0-\tilde{v}_1)/\Delta Y \\ &\text{Corrector level:} \quad \tilde{v}_Y \approx (2\tilde{v}_0-3\tilde{v}_1+\tilde{v}_2)/\Delta Y \end{aligned}\right\} \tag{89}$$

with

$$\tilde{v}_0=\tilde{v}(o,Y) \ , \ \tilde{v}_1=\tilde{v}(o,Y-\Delta Y) \ , \ \tilde{v}_2=\tilde{v}(o,Y-2\Delta Y) \tag{90}$$

5) For the same reason, that is, for a better evaluation of Lagrangian derivatives in the momentum equations, the values of u_X, v_X, u_Y, v_Y in the second and third of (28) should be approximated following the same rule as described by (87).

6) Y-derivatives at the bow shock are conveniently approximated by centered differences, except for c_Y at the last two points, where two-point backward differences are used (Ref. 4).

10. Equations of Motion for the Afterbody Flow

In studying the steady, supersonic, axisymmetric flow in the shock layer, we may start again from (17), after dropping the time derivatives, and introducing an angular variable,

$$\sigma = \frac{v}{u} \tag{91}$$

After some algebraic manipulations, the following set of equations is obtained:

$$\varkappa P_\xi+\sigma P_\eta+\gamma[\sigma_\eta-(1+\sigma^2)\ \frac{G_\xi}{G}+j\ \frac{V}{Gyu}] = 0$$

$$\sigma_\xi+\sigma\sigma_\eta+\frac{\mathcal{J}}{u^2}(P_\eta-\sigma P_\xi)+(1+\sigma^2)\left(\frac{G_\eta}{G}-\sigma\ \frac{G_\xi}{G}\right) = 0 \qquad (92)$$

$$S_\xi+\sigma S_\eta = 0$$

where

$$\varkappa = 1 - \frac{a^2}{u^2} \qquad (93)$$

These are the only equations which require integration since, for a steady, isenergic flow,

$$q^2 = \frac{2\gamma}{\gamma-1}(\mathcal{J}_o-\mathcal{J}) \qquad (94)$$

where $\mathcal{J}_o$ is the stagnation value of $\mathcal{J}$, and, in turn,

$$\mathcal{J} = \exp\left(\frac{\gamma-1}{\gamma}P+\frac{1}{\gamma}S\right) \qquad (95)$$

If the same stretching function as in Section 4 is used, and X is given the same meaning, but T is now made equal to ξ, we may use the following definitions in order to maintain our present notation as close as possible to the one used in Ref. 1:

$$A = X_\xi+\frac{\sigma}{\varkappa}X_\eta\ ,\ B = X_\xi+\sigma X_\eta \qquad (96)$$

$$C=X_\eta-\sigma X_\xi\ ,\ D=(1+\sigma^2)\varphi_1-j\ \frac{V}{Gyu}\ ,\ E=(1+\sigma^2)(\sigma\varphi_1+\varphi_2) \qquad (97)$$

Since, for any function, F:

$$F_\xi=F_T+F_X X_\xi\ ,\ F_\eta=F_X X_\eta \qquad (98)$$

the system (92) becomes:

$$\left.\begin{aligned} &P_T+AP_X+\frac{\gamma}{\varkappa}(X_\eta\sigma_X-D)=0\\ &\sigma_T+B\sigma_X+\frac{\mathcal{J}}{u^2}(CP_X-\sigma P_T)-E=0\\ &S_T+BS_X=0 \end{aligned}\right\} \qquad (99)$$

Eqs. (29) must be replaced by

$$\xi_X=0\ ,\ \xi_T=1\ ,\ \eta_X=1/X_\eta\ ,\ \eta_T=-X_\xi/X_\eta\ . \qquad (100)$$

11. Characteristic Equation for the Steady Flow Problem.

Body Calculation

To evaluate points on the body or on the bow shock, a characteristic equation in X and T, obtained from the first two equations (99), is needed, in the form of a linear combination:

$$(\mu_1-\sigma\frac{\mathcal{J}}{u^2}\mu_2)(P_T+\lambda P_X)+\mu_2(\sigma_T+\lambda\sigma_X)=\frac{\gamma}{\varkappa}D\mu_1+E\mu_2 \qquad (101)$$

whose λ is defined by

$$\lambda=B+\frac{a^2}{\varkappa u^2}X_\eta[\sigma\pm\beta]\ ,\quad \beta^2=(1+\sigma^2)\frac{u^2}{a^2}-1 \qquad (102)$$

and, consequently,

$$\mu_1=B-\lambda\ ,\ \mu_2=-\frac{\gamma}{\varkappa}X_\eta\ ,\ \mu_1-\sigma\frac{\mathcal{J}}{u^2}\mu_2=\mp\frac{a^2}{\varkappa u^2}X_\eta\beta \qquad (103)$$

At the body, the lower sign must be used; in addition, B=0. From (37),

$$\sigma=b_\xi \qquad (104)$$

and

$$\sigma_T=\sigma_\xi+\sigma_\eta\eta_T = b_{\xi\xi} \tag{105}$$

Therefore, the equation (101) defining the pressure at the body becomes:

$$P_T= - \lambda P_X+ \frac{u^2}{\delta\mathcal{J}}(b_{\xi\xi}+\lambda\sigma_X-E) - \frac{\gamma}{\kappa\beta}(\sigma-\beta)D \tag{106}$$

Obviously, b_ξ and $b_{\xi\xi}$ will be evaluated according to (43) and (44).

12. Bow Shock Calculation for the Steady State Problem

Equations (45) and (46) still hold, as well as (49). By writing c' and c'' in lieu of c_ξ and $c_{\xi\xi}$, respectively, we have now:

$$\nu_T=c'c''/\nu \ , \ N_{2T} =- c'c''/\nu^3 \ , \ N_{1T}=- c''/\nu^3 \tag{107}$$

The basic unknown is still c_{TT}, that is, c''. To determine it, we note first that

$$\tilde{u}_\infty = u_\infty N_1+v_\infty N_2 \tag{108}$$

Then,

$$\tilde{u}_{\infty T}= u_{\infty T}N_1+v_{\infty T}N_2+u_\infty N_{1T}+v_\infty N_{2T}$$

$$= U_\infty (\mathcal{C}_T N_1 - \mathcal{S}_T N_2 - \mathcal{C}c''/\nu^3 + \mathcal{S}c'c''/\nu^3)$$

but

$$\mathcal{C}_T+i\mathcal{S}_T= -ie^{-i\omega}(\omega_\xi+\omega_\eta c') =-ie^{-i\omega}(\varphi_2+c'\varphi_1)$$

so that

$$\tilde{u}_{\infty T} = (-v_\infty N_1 + u_\infty N_2)(\varphi_2 + c'\varphi_1) - (u_\infty + c'v_\infty)c''/\nu^3 \qquad (109)$$

We will then write

$$\tilde{u}_{\infty T} = C_1 c_{TT} + C_2 \qquad (110)$$

with

$$C_1 = -(u_\infty + c'v_\infty)/\nu^3 \qquad (111)$$

$$C_2 = (-v_\infty N_1 + u_\infty N_2)(\varphi_2 + c'\varphi_1) = -C_1 \nu^2 (\varphi_2 + c'\varphi_1) \qquad (112)$$

Since (62) and (63) still hold, with $\tilde{u}$ and $\tilde{u}_\infty$ in lieu of $\tilde{u}_{rel}$ and $\tilde{u}_{\infty rel}$, respectively, it follows that Eqs. (64) through (68) are valid. Eqs. (70) and (71) are also valid. So are (72) and (73); therefore, (74) can still be used, provided that C_{11}, C_{12}, C_{13}, C_{14} are redefined as follows:

$$\left.\begin{aligned} C_{11} &= C_9 N_1 - (\tilde{u} - \tilde{u}_\infty)/\nu^3 \\ C_{13} &= C_9 N_2 - (\tilde{u} - \tilde{u}_\infty)c'/\nu^3 \end{aligned}\right\} \qquad \left.\begin{aligned} C_{12} &= -v_\infty(\varphi_2 + c'\varphi_1) + C_{10} N_1 \\ C_{14} &= u_\infty(\varphi_2 + c'\varphi_1) + C_{10} N_2 \end{aligned}\right\} \qquad (113)$$

Consequently,

$$\sigma_T = C_{15} c_{TT} + C_{16} \qquad (114)$$

with

$$\left.\begin{aligned} C_{15} &= (C_{13} - \sigma C_{11})/u \\ C_{16} &= (C_{14} - \sigma C_{12})/u \end{aligned}\right\} \qquad (115)$$

We use now the characteristic equation (101) with the upper sign in the definition of λ; by letting:

$$D_7 = 1/(\mathcal{J}\beta C_3 + C_{1\beta} u^2)$$

$$D_8 = \mathcal{J}\beta C_4 + C_{1\beta} u^2$$

$$D_9 = u^2 (\omega_1 D/X_\eta - E) \qquad (116)$$

$$\pi = \lambda (\mathcal{J}\beta P_X + u^2 \sigma_X)$$

the following equation is obtained, to define c_{TT}:

$$c_{TT} = -D_7 (D_8 + D_9 + \pi) \qquad (117)$$

This equation is formally the same as (78).

13. Outline of the Computational Program for the Afterbody Flow

Initial conditions for a marching integration technique are the converged steady values on the next to the last ξ=constant line of the blunt body flow calculation.

Each computational step consists of a predictor level and a corrector level.

Predictor level

Given original values of P, σ, $\mathcal{J}$, S, c, c_T, z, ζ, g and φ (at a constant ξ),

compute the X-derivatives of P, σ, S,

compute X_ξ and X_η,

compute G, A, B, C, D, E.

For all points except the body point and the shock point, determine P_T, σ_T and S_T from (99).

For body points, determine P_T from (106) and let $S_T=0$.

For shock points, compute all the coefficients (C_1 through C_{18}, D_7, D_8, D_9, π) necessary to determine c_{TT} from (117).

Update P, S and σ at all interior points, P and S at the body and c and c_T using (82).

With the new value of T, that is, $T=\xi+\Delta\xi$, new values of b, b_ξ and $b_{\xi\xi}$ are evaluated, and an updated σ at the body is taken equal to b_ξ.

Moreover, a new grid line is obtained, extending from b to the updated value of c. New grid points are determined and the updated values of P, S and σ are affixed to them.

At the new shock point, the new value of c_T is used to evaluate a new normal and then (62), (63), (81), (72) and (91) determine P, S, and σ behind the shock. Values of $\mathcal{J}$ are obtained throughout from (95) and values of u from (94) and

$$u^2 = q^2/(1+\sigma^2) \tag{118}$$

The new values of P, S, σ, c, and c_T are temporarily saved.

At the new grid points, g and φ are computed.

Corrector level

The computation is restarted as in the predictor stage, using all new values. The updating is performed using (84). The computational grid must be re-evaluated after correcting c. Finally, the updated values of P, S, $\mathcal{J}$, σ, c, and c_T are stored as initial values for a new step.

14. Mapping Technique

The preceding analysis holds, regardless of the technique used to generate the computational grid. In the current series of tests, a very simple mapping technique was used, suggested by D. Hall* in a private communication. The technique is easier to analyze and to code than the one originally considered, which was a byproduct of the method I developed for three-dimensional calculations of supersonic flows (Refs. 1 and 5). The original mapping maintains the geometrical symmetry about the body axis, if the body is symmetrical, whereas the present one does not. If the body is not symmetrical, and for three-dimensional problems in general, conservation of symmetry trhoughout the mapping seems not to be a necessary requirement. In the current series of tests, where symmetry is still a typical feature of the flow, loss of symmetry in the calculation of the blunt body flow seems not to affect the results.

A number of "hinge-points" are selected inside the body, to represent a coarse skeleton of the body itself. Let J be the total number of hinge-points, the first of which lies on the x-axis, in the vicinity of the body stagnation point. Let us consider a succession of J+1 planes, called the z_j-planes (j=1, J+1), the first of which is identical with the original physical plane (the z-plane), so that

*General Electric Co., Valley Forge, Pa.

$$z_1 = z$$

All these planes are related to each other in a similar way, that is, through the general function:

$$z_{j+1} = 1+(z_j - h_{jj})^{\delta_j} \tag{119}$$

where h_{jj} is the image of the j-th hinge-point in the z_j-plane, and δ_j is defined as

$$\delta_j = \frac{\pi}{\delta - \arg(h_{j+1,j} - h_{jj})} \tag{120}$$

where $h_{j+1,j}$ is the image of the (j+1)-th hinge-point in the z_j-plane. Since all points of interest (including the hinge-points) lie in the upper half of the z-plane, the set of hinge-points will finally result aligned along the real axis of the z_{J+1}-plane. Note that the image of the x-axis to the left of the first hinge-point will result into a portion of the real axis on the z_{J+1}-plane, to the left of the image of the first hinge-point $(h_{1,J+1})$. Note also that, with the exception of the first, straight segments in the z-plane between two successive hinge-points are not mapped onto straight segments in the z_{J+1}-plane.

For each partial mapping, let

$$g_j = \frac{dz_{j+1}}{dz_j} = \delta_j \frac{z_{j+1}^{-1}}{z_j - h_{jj}} \tag{121}$$

A final mapping is then applied, of the form:

$$\zeta = \sqrt{z_{J+1} - h_{J+1,J+1}} \tag{122}$$

for which

$$\frac{d\zeta}{dz_{J+1}} = \frac{1}{2\zeta} \tag{123}$$

In the ζ-plane, the image of the body becomes a line defined by an almost constant value of η, starting at $\xi=0$, whereas the portion of the x-axis in front of the body becomes a portion of the imaginary axis. From (121) and (123) it follows that

$$g = \frac{1}{2\zeta} \prod_{j=1}^{J} g_j \tag{124}$$

According to the defnition (8),

$$\varphi = \frac{1}{g}\left[-\frac{g}{\zeta} + \sum_{j=1}^{J} \frac{1}{g_j} \frac{dg_j}{dz} \right]$$

$$= -\frac{1}{\zeta} + \frac{1}{g} \sum_{j=1}^{J} \frac{1}{g_j} \frac{dg_j}{dz_j} \prod_{\ell=0}^{j-1} g_\ell \qquad (g_o=1)$$

and, since

$$\frac{dg_j}{dz_j} = \frac{\delta_j - 1}{z_j - h_{jj}} g_j$$

it follows that

$$\varphi = -\frac{1}{\zeta} + \frac{1}{g} \sum_{j=1}^{J} \frac{\delta_j - 1}{z_j - h_{jj}} \prod_{\ell=0}^{j-1} g_\ell \tag{125}$$

15. Results of Test Calculations

We report here results for the following test calculations:

Case No.	1	3	4	5	6	7
Free stream Mach number	3	4	4	4	4	4
Flow (two-dimensional or axisymmetric)	2-D	2-D	A-S	2-D	A-S	A-S
Body geometry	parabola	sphere-cylinder		sphere-cone		see Fig. 9
Location of hinge-points in physical plane	-0.75 2	-0.9 -0.63(1-i) 0.9i 3+0.9i				-0.9 -0.63(1-i) 2+1.1i 4
Number of intervals in blunt body calculation	5x12	6x6	6x6	6x6	6x6	6x7
Number of intervals in afterbody calculation	10	24	24	24	24	24

Stretching is not used in any of the preceding cases. In case No. 8, the same data are used as in case 6 but a strong stretching, with $\alpha=2$ and 12 intervals between shock and body, is used. Fig. 1 shows the grids as they appear in the physical plane in both cases, for comparison. Figs. 2 through 8 show isobars as computed. Note that there is no difference between Fig. 6 and Fig. 8. Finally, Fig. 9 shows some lines from the grid for case 7, to demonstrate the ability of the mapping to adjust to bodies of unusual shape.

All calculations were performed on Polytechnic's IBM 360/65. Their success is due to the dedicated cooperation of Miss Catherine Fahy, without whose help I would not have been able to get my

program to operate on the machine's extremely complicated system.

16. References

1. Moretti, G.: "Calculation of the Three-Dimensional, Supersonic, Inviscid, Steady Flow Past an Arrow-Winged Airframe, Part I". Polytechnic Institute of New York, POLY-AE/AM Report No. 76-8, May 1976.

2. MacCormack, R.W.: "The Effect of Viscosity in Hyper-velocity Impact Cratering". AIAA Paper No. 69-354, 1969.

3. Moretti, G.: "Circumspect Exploration of Multidimensional Imbedded Shocks". AIAAJ., 14, pp. 894-899, 1976.

4. Moretti, G.: "A Pragmatical Analysis of Discretization Procedures for Initial- and Boundary-Value Problems in Gas Dynamics and Their Influence on Accuracy, or: Look Ma, No Wiggles!" Polytechnic Institute of New York, POLY-AE/AM Report No. 74-15, September 1974.

5. Moretti, G.: "Conformal Mappings for Computations of Steady, Three-Dimensional, Supersonic Flows". Numerical/Laboratory Computer Methods in Fluid Mechanics, ed. by A.A. Pouring and V.I. Shah, American Society of Mechanical Engineers, N.Y., pp. 13-28, 1976.

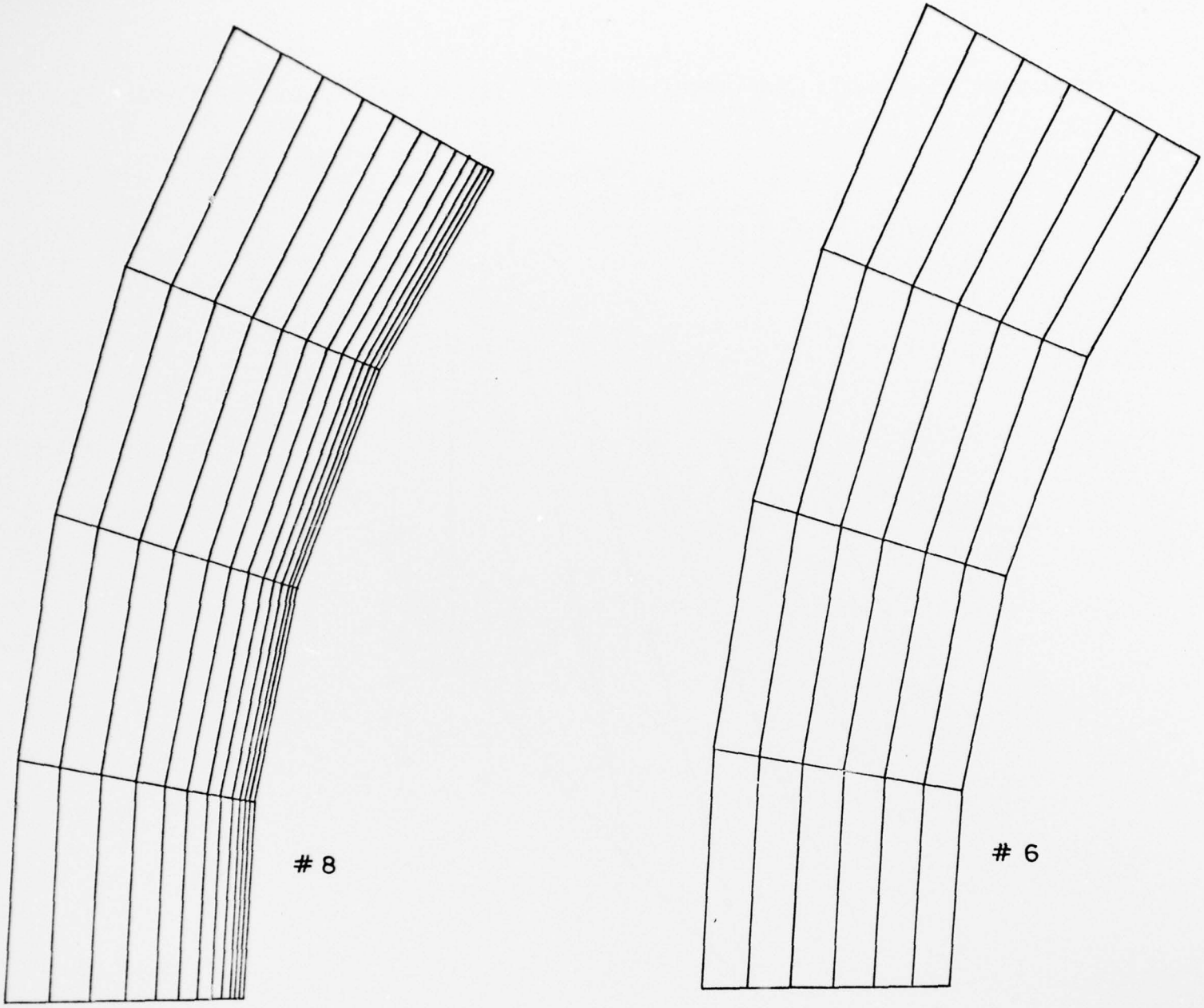

FIG. 1. COMPUTATIONAL GRIDS FOR RUNS #8 AND 6

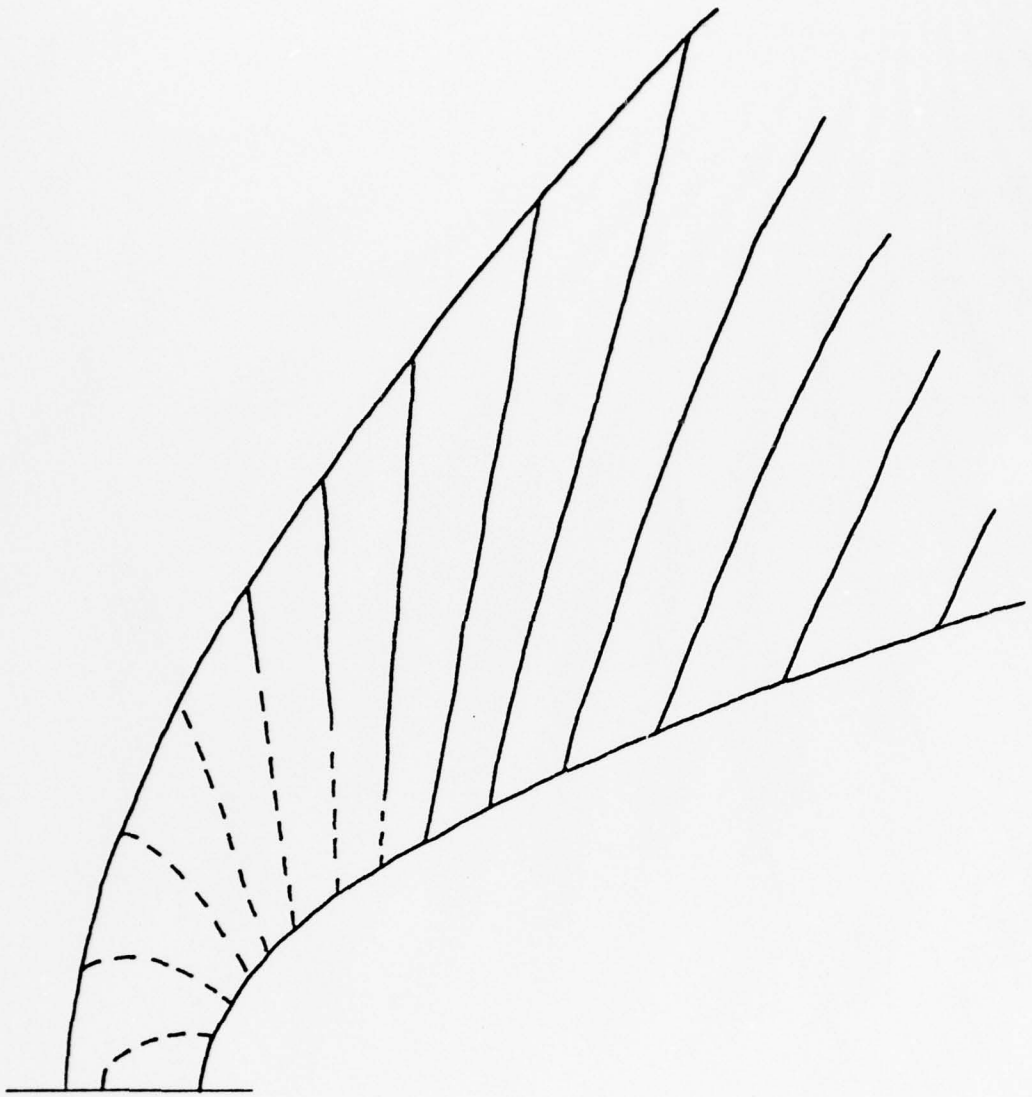

FIG. 2. ISOBARS FOR RUN #1. (BROKEN LINES FROM BLUNT BODY ANALYSIS)

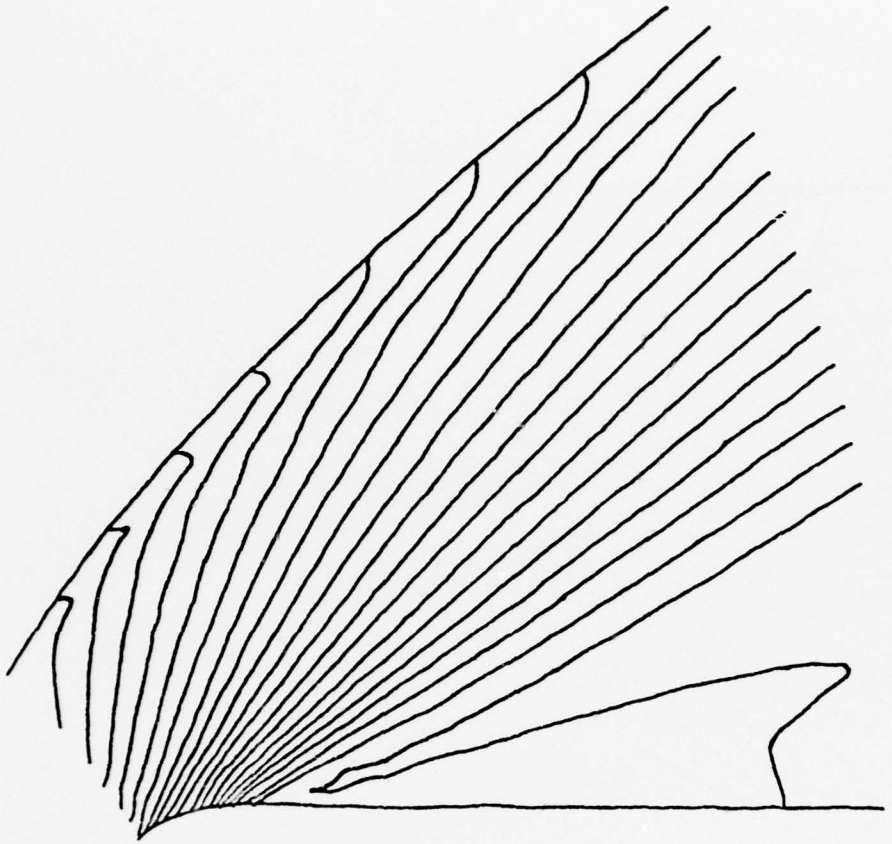

FIG. 3. ISOBARS FOR RUN #3

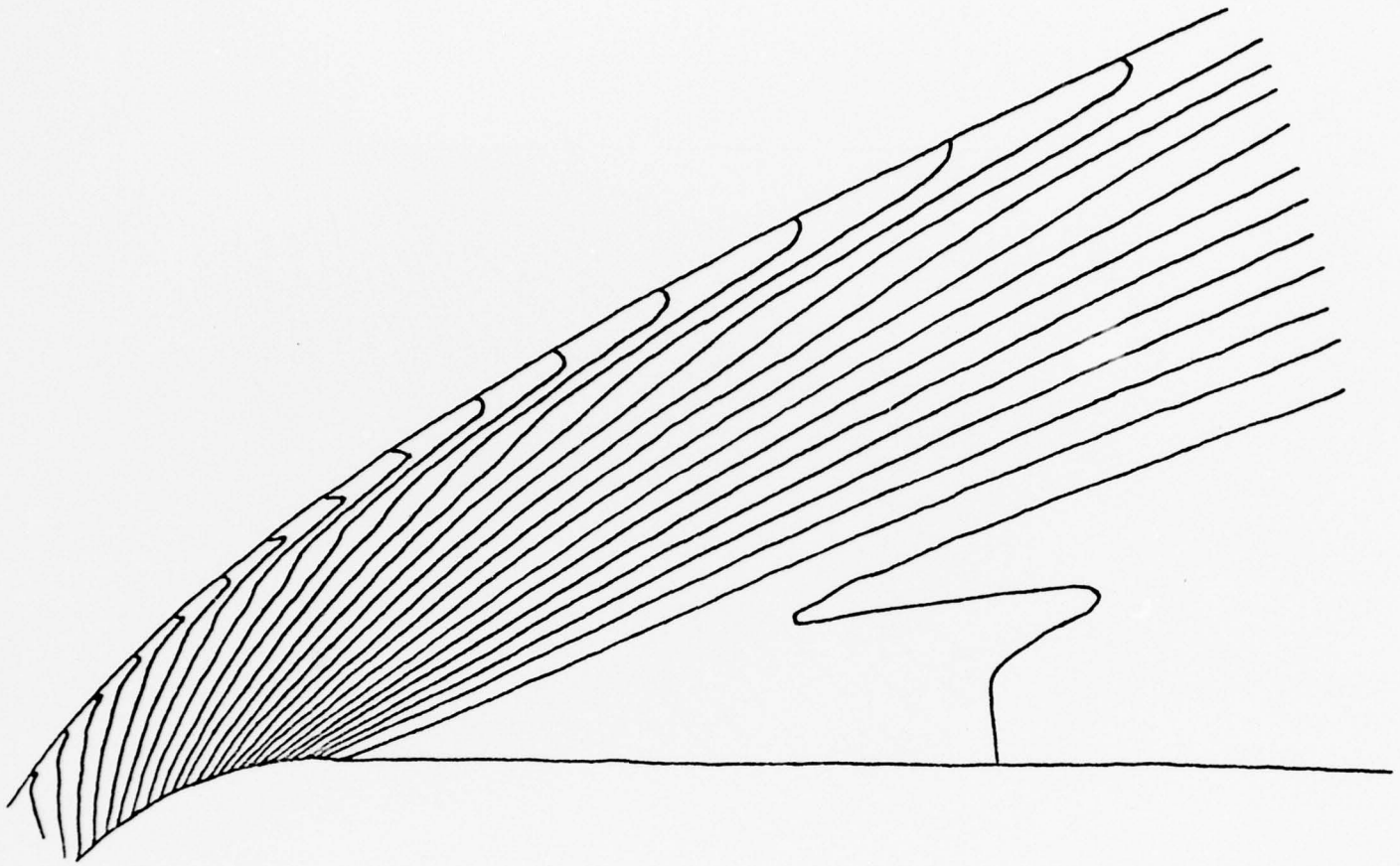

FIG. 4. ISOBARS FOR RUN #4

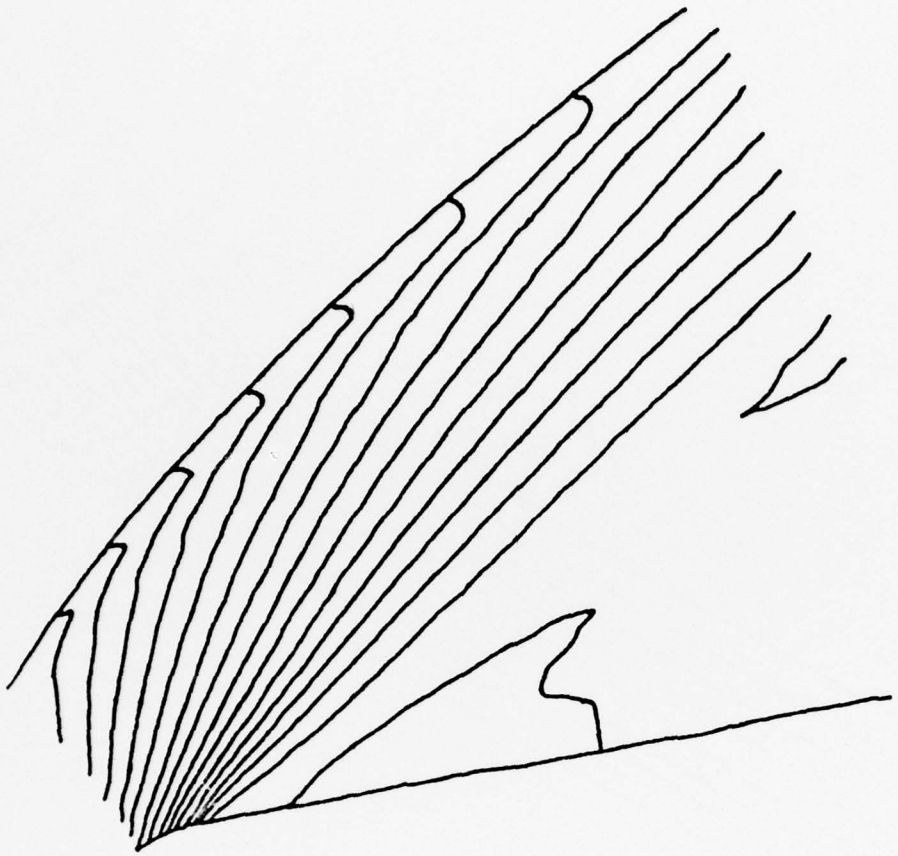

FIG. 5. ISOBARS FOR RUN #5

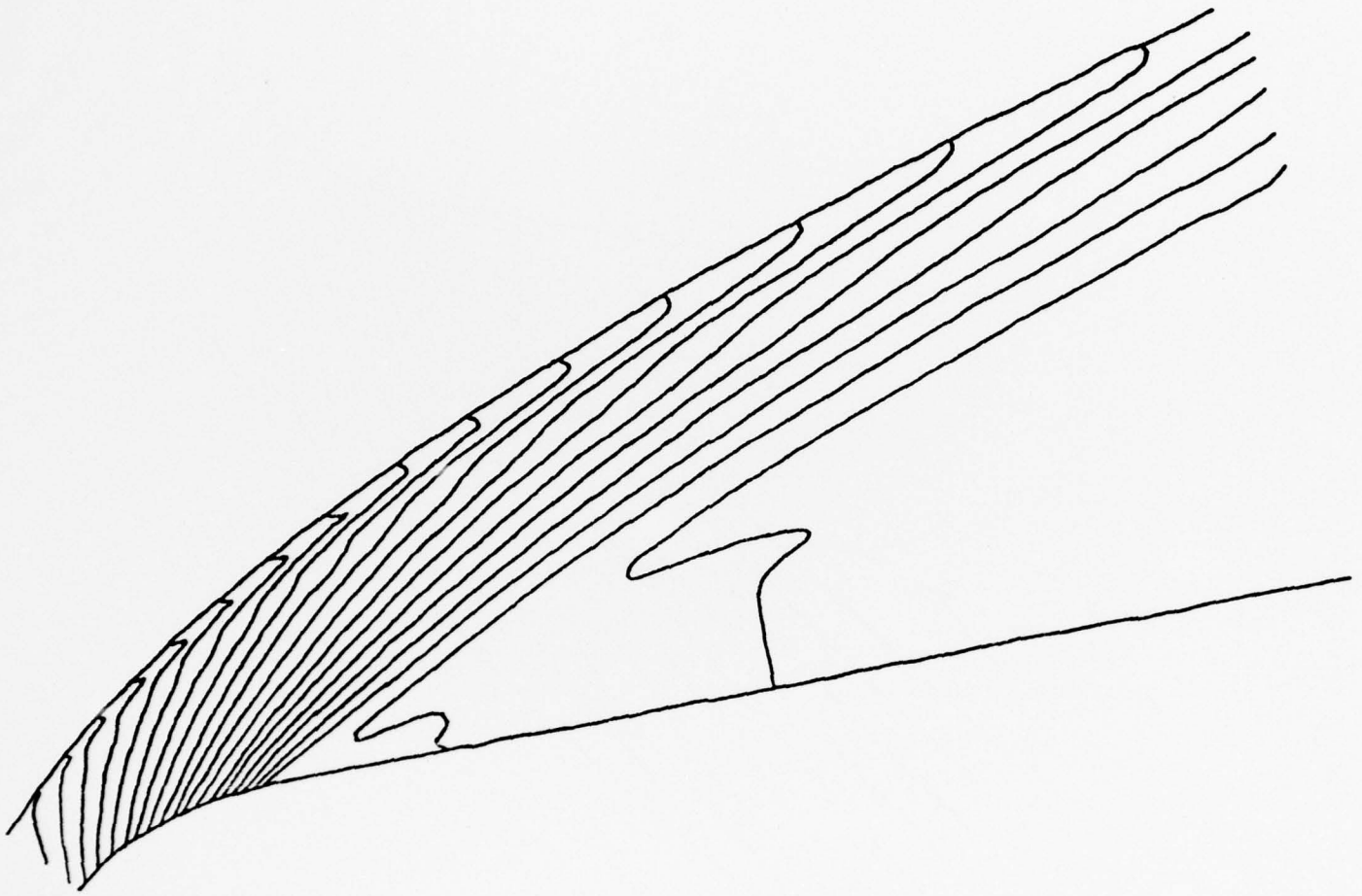

FIG. 6. ISOBARS FOR RUN #6

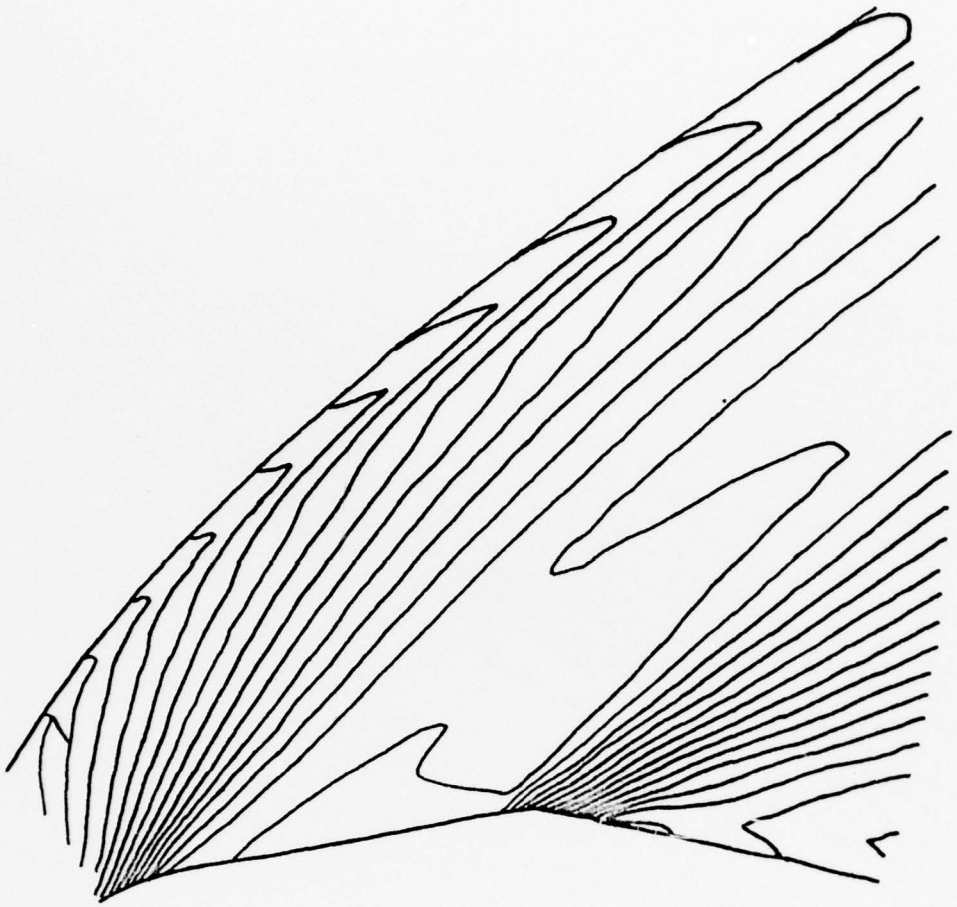

FIG. 7. ISOBARS FOR RUN #7

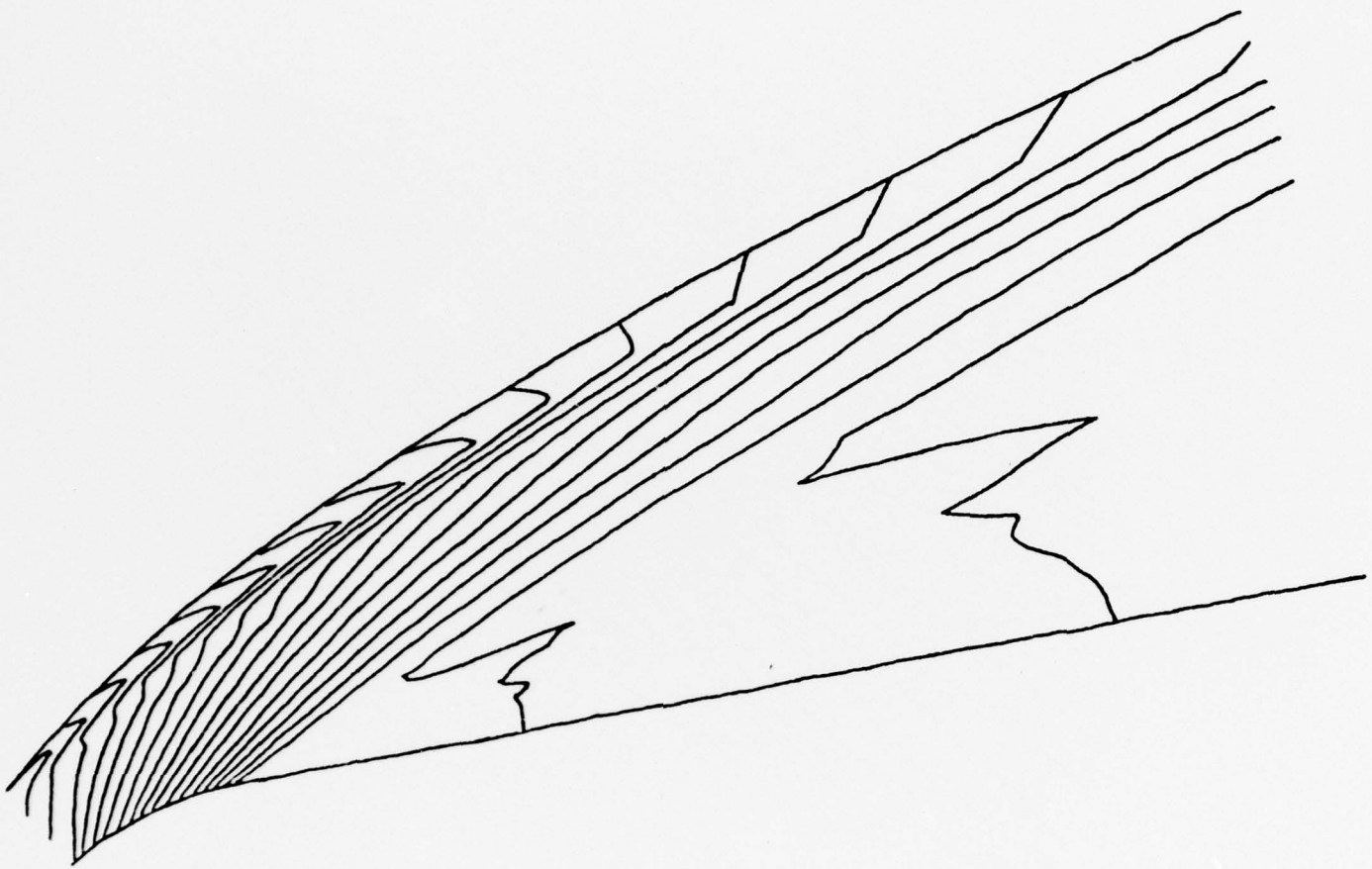

FIG. 8 - ISOBARS FOR RUN #8

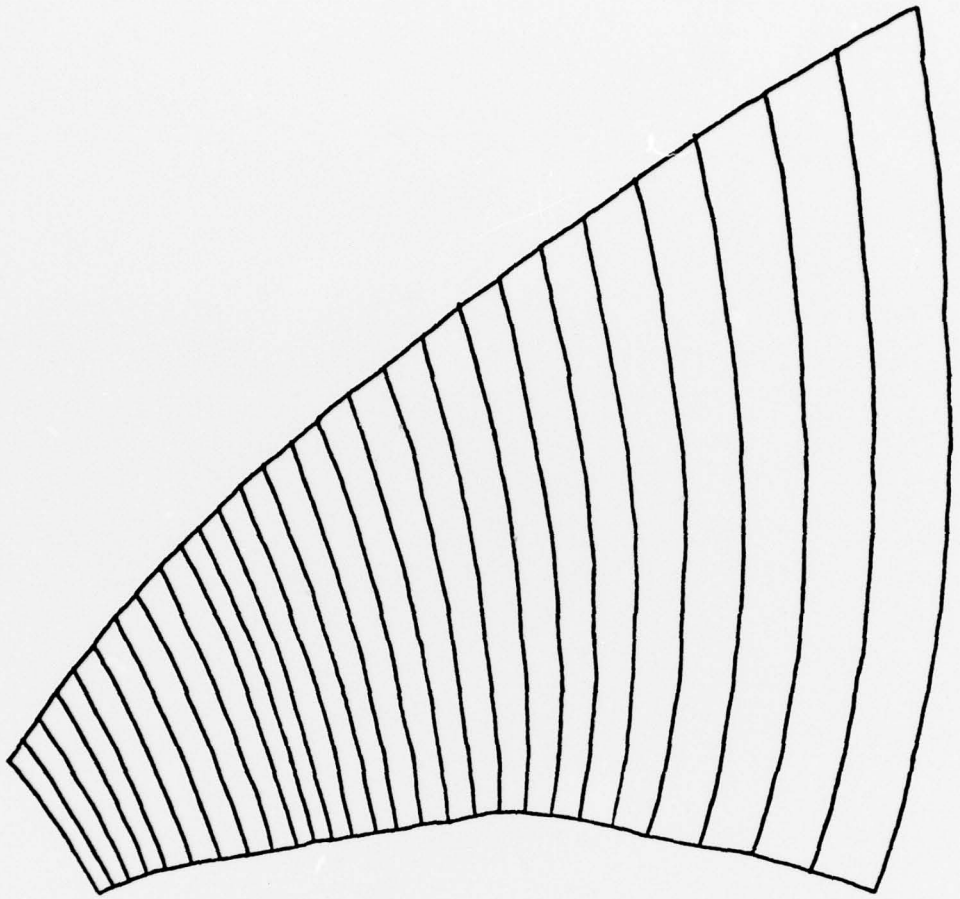

FIG. 9. SAMPLE OF COMPUTATIONAL GRID FOR RUN #7